Combining chemical genetics and proteomics to identify protein kinase substrates

Noah Dephoure*†‡, Russell W. Howson*†, Justin D. Blethrow§, Kevan M. Shokat§, and Erin K. O'Shea*‡¶

*Howard Hughes Medical Institute and Departments of Biochemistry and Biophysics and §Cellular and Molecular Pharmacology, University of California, San Francisco, CA 94143

Phosphorylation is a ubiquitous protein modification important for regulating nearly every aspect of cellular biology. Protein kinases are highly conserved and constitute one of the largest gene families. Identifying the substrates of a kinase is essential for understanding its cellular role, but doing so remains a difficult task. We have developed a high-throughput method to identify substrates of yeast protein kinases that employs a collection of yeast strains each expressing a single epitope-tagged protein and a chemical genetic strategy that permits kinase reactions to be performed in native, whole-cell extracts. Using this method, we screened 4,250 strains expressing epitope-tagged proteins and identified 24 candidate substrates of the Pho85–Pcl1 cyclin-dependent kinase, including the known substrate Rvs167. The power of this method to identify true kinase substrates is strongly supported by functional overlap and colocalization of candidate substrates and the kinase, as well as by the specificity of Pho85–Pcl1 for some of the substrates compared with another Pho85-cyclin kinase complex. This method is readily adaptable to other yeast kinases.

cell signaling | phosphorylation | cyclin-dependent kinase

The general criteria for establishing that a protein is a substrate of a given kinase are the ability of the kinase to phosphorylate the substrate *in vitro* and the dependence on the activity of the kinase for phosphorylation of the substrate *in vivo* (1). *In vivo* validation of kinase substrates continues to be laborious and time-consuming. Thus, it is crucial to be able to efficiently identify candidates before committing to this step. Indirect data, such as genetic and physical interactions, can provide insights into potential substrates, but many interacting proteins and genes are not substrates (1, 2). More direct approaches using *in vitro* kinase reactions have been attempted in many permutations (1, 2). Purified component reactions directly measure the ability of a kinase to phosphorylate a particular substrate and can be scaled for high-throughput formats, but such conditions often compromise reaction specificity and produce false-positive results (1, 2).

We sought to improve on these techniques by carrying out a biochemical screen in an environment that more closely resembles the *in vivo* state. To do so, we carried out kinase reactions with near physiological levels of exogenous kinase in native whole-cell extracts. These extracts maintain protein–protein interactions that may affect substrate presentation and preserve a nearly full complement of cellular proteins, including potential adaptor proteins and cofactors that could affect the reaction. These reaction conditions also preserve the native relative protein abundances and a natural competition among substrates for limited kinase.

A challenge of carrying out protein kinase reactions in whole-cell lysates is that one cannot attribute phosphorylation of a protein to a particular kinase in the reaction, because all kinases in the extract are capable of catalyzing phosphotransfer. To permit us to assign phosphorylation of a protein to a particular protein kinase, we made use of a chemical genetic strategy using a mutant kinase, analog specific (AS), whose nucleotide binding specificity is altered to allow it to use a modified form of ATP

(3). An AS version of a kinase is generated by replacing a conserved, bulky hydrophobic group in the ATP-binding pocket with a smaller residue, allowing the AS kinase to use an ATP analog that fits into the engineered "hole" in the ATP-binding pocket. In an assay using an AS kinase and a radiolabeled ATP analog, all radiolabeled proteins are necessarily phosphorylated by the mutant kinase, because no other kinase can efficiently use the analog. This chemical genetic approach has been applied to identify substrates of v-Src by carrying out a kinase reaction in a cell lysate and identifying radiolabeled protein bands by using mass spectrometric approaches (4). A difficulty with this strategy is that the dynamic range of protein abundance makes it difficult to identify low-abundance substrates. More recent studies in budding yeast have circumvented these identification problems by combining this chemical genetic approach with a protein expression library. Cdk1 substrates were identified by screening a set of candidate proteins containing the Cdk1 consensus phosphorylation sequence, which were overexpressed as fusions to glutathione *S*-transferase (GST) (5). The success of this approach motivated us to develop a systematic unbiased strategy that permits screening for substrates of kinases with no known consensus target sequence and that uses proteins present at their natural levels of abundance. Our screen makes use of a collection of yeast strains we generated in which each strain produces a single epitope-tagged protein expressed from its native chromosomal locus, under the control of the endogenous promoter (6, 7). To identify substrates, we generated extracts from these strains, carried out kinase reactions in the extracts by adding AS kinase and radiolabeled ATP analog, isolated the epitope-tagged proteins by immunopurification, resolved the immunocomplexes on a gel, and assayed for the incorporation of the radiolabel.

As a test of this method, we screened for substrates of Pho85, a nonessential yeast cyclin-dependent kinase (8). Pho85, when bound to the cyclin Pho80, plays a well characterized role in the cellular response to phosphate starvation (8, 9). However, cells lacking *PHO85* have additional phenotypes unrelated to the phosphate starvation pathway (10, 11). Ten different Pho85 cyclins, termed Pcls, have been shown to associate with Pho85 and are thought to direct it to phosphorylate distinct substrates involved in different cellular processes (12, 13). To better understand the role of the Pho85–Pcl1 cyclin-dependent kinase, we undertook a systematic screen of the yeast proteome for substrates, making use of an AS version of Pho85, Pho85(F82G),

which functionally substitutes for wild-type Pho85 *in vivo*, and which is able to use the ATP analog N^6-benzyl-ATP *in vitro* (14).

Materials and Methods

Yeast Strains. All strains are derivatives of BY4741 (available from American Type Culture Collection) and are from the epitope-tagged fusion library described in refs. 6 and 7 (available from Open Biosystems, Huntsville, AL).

Protein Purification. Purification of Pho85–cyclin complexes was performed as described in ref. 15. Briefly, expression plasmids for Pho85(F82G)-6His (EB1375) and either Pho80 (EB1076) or Pcl1 (EB1613) were cotransformed into BL21 DE3 *Escherichia coli*, induced with 200 μM isopropyl β-D-thiogalactoside for 6 h, pelleted, and frozen. The cell lysate was loaded on a Ni^{2+} charged iminodiacetic acid HiTrap chelating HP column (GE Healthcare, Buckinghamshire, U.K.) and washed, and the protein complexes were eluted with imidazole. Dimeric cyclin-dependent kinase (CDK) was purified away from CDK monomer on a Superose 12 size-exclusion column. Purified kinase concentrations were determined by using calculated extinction coefficients and by measuring UV absorption in 6 M guanidine·hydrochloride (16). Kinase activity was confirmed with *in vitro* reactions using a Pho4-peptide substrate and/or full-length Pho4. The purification of Pho4 and Pho4-zz has been described in refs. 17 and 18.

ATP Analog Synthesis. N^6-benzyl-[γ-^{32}P]ATP was prepared enzymatically from N^6-benzyl-ADP by using a modified version of the protocol described in ref. 19. Two hundred microliters of a 1:1 slurry of Co^{2+}-charged iminodiacetic acid-Sepharose beads in Hepes-buffered saline (HBS) (50 mM Hepes, pH 7.4/150 mM NaCl) were added to an empty 2-ml BioSpin column (Bio-Rad) and washed twice with 1 ml of HBS. Five hundred micrograms of 10-His-tagged nucleoside 5′-diphosphate kinase (NDPK), purified from *E. coli*, was added in 1 ml of HBS. The column was washed once with 1 ml of PBS, pH 7.5. The NDPK was allowed to autophosphorylate by adding 5 mCi (1 Ci = 37 GBq) of end-labeling grade [γ-^{32}P]ATP (MP Biomedicals, Irvine, CA) in 1 ml of PBS (137 mM NaCl/2.7 mM KCl/10 mM Na_2HPO_4/1.76 mM KH_2PO_4, pH 7.4) and washed twice with PBS. Twenty-five nanomoles of N^6-benzyl-ADP (19) was added in 80 μl of PBS containing 10 mM $MgCl_2$. NDPK catalyzes transfer of the [^{32}P]phosphate to the N^6-benzyl-ADP, producing γ-^{32}P-labeled N^6-benzyl-ATP. The final product was eluted with 250 μl of PBS with $MgCl_2$. *para*-Aminobenzoic acid was added to 50 mM final concentration as a stabilizer, and the product was stored at 4°C. Product activity and efficiency were monitored by scintillation counting of flow-through fractions. We routinely recovered >40% of total activity in the final product.

Cell Growth and Yeast Extract Preparation. Individual tandem affinity purification (TAP)-tagged strains were inoculated from fresh overnight, saturated cultures into 1.8 ml of yeast extract/peptone/dextrose (YEPD) in deep-well 96-well plates (Greiner, Longwood, FL) at $OD_{600} \approx 0.2$–0.3 and grown to late-logarithmic phase ($0.8 < OD_{600} < 1.0$) at 30°C in a HiGro growth chamber (Genomic Solutions, Ann Arbor, MI). The cells were pelleted and resuspended in 150 μl of sorbitol buffer (SB) [1.2 M sorbitol/0.1 M KH_2PO_4, pH 7.4/2 μl/ml 2-mercaptoethanol (β-ME)]. Pellets from six plates were combined, pelleted, resuspended in 150 μl of SB along with 15 μl of lyticase (20), and transferred to a 96-well PCR plate. Lyticase treatment proceeded at 30°C for 15 min on a thermal cycler. Cells were then chilled on ice, pelleted, and washed once with 150 μl of SB without β-ME, frozen in liquid nitrogen, and stored at −80°C. To lyse the spheroplasted cells, pellets were thawed on ice and resuspended in 105 μl of ice-cold hypotonic lysis buffer (50 mM

Tris·HCl, pH 7.5/5 mM $MgCl_2$/5 mM EGTA/1 mM EDTA/0.1% Triton X-100/2 mM PMSF/2.5 mM benzamidine/1 μg/ml pepstatin A/1 μg/ml leupeptin/1 mM β-ME). After a 10-min incubation on ice, we added 21 μl of hypotonic lysis buffer with 0.9 M NaCl (final NaCl concentration = 150 mM), followed by an additional 10-min incubation on ice. Lysates were cleared by centrifugation for 45 min at 5,000 × *g* at 4°C. One hundred microliters of supernatant was transferred to a 1-ml deep-well 96-well plate containing 25 μl of 50% glycerol. Lysates were frozen in liquid nitrogen and stored at −80°C. We routinely sampled extracts and measured the total protein concentration by Bradford assay. Protein concentrations were typically ≈10 mg/ml. The manipulation of cells and lysates in 96-well format was performed by using a Biomek FX robot (Beckman).

High-Throughput Kinase Reactions. Reaction solutions were prepared in three parts: the substrate extract, a 3× kinase solution, and a 3× reaction solution with the radiolabeled ATP analog. Extracts were thawed on ice, and the components were allowed to come to room temperature before the reactions were started by adding 120 μl of 3× kinase solution [30 nM Pho85(F82G)–Pcl1/0.65 mg/ml pyruvate kinase (Roche)/50 mM Tris·HCl, pH 7.5/150 mM NaCl/10% glycerol/0.1 mg/ml BSA (Roche)/1 mM β-ME/0.1% Nonidet P-40/2 mM PMSF/2.5 mM benzamidine] followed by 120 μl of 3× reaction mix [200 mM Tris·HCl, pH 7.5/150 mM NaCl/10% glycerol/120 mM phospho*enol*pyruvic acid (Sigma)/160 mM β-glycerophosphate/30 mM NaF/3 mM ATP/10 mM EGTA/0.3 mg/ml BSA/25 mM $MgCl_2$/300 nM calyculin A/30 μCi of N^6-benzyl-[γ-^{32}P]ATP]. Reactions proceeded for 15 min at 25°C with occasional gentle vortexing and were stopped by the addition of 200 μl of ice-cold IP buffer (50 mM Tris·HCl, pH 7.5/300 mM NaCl/5 mM $MgCl_2$/5 mM EGTA/1 mM EDTA/1% Triton X-100/160 mM β-glycerophosphate/2 mM β-ME/10 mM NaF/1 mM activated Na_3VO_4/2 mM PMSF/2.5 mM benzamidine/1 μg/ml pepstatin A/1 μg/ml leupeptin) with 3 μg biotin-SP-conjugated human IgG (Jackson ImmunoResearch) and incubated for 30 min at 4°C. About 5 μl of packed volume streptavidin-Sepharose (GE Healthcare) was added in 40-μl total volume of IP buffer. The samples were incubated for an additional 90 min at 4°C with occasional light vortexing and transferred to a 96-well fritted filter plate (Orochem Technologies, Lombard, IL; no. OF 1100) on a vacuum manifold. The beads were washed four times with 400 μl of IP buffer. After the final wash, residual buffer was removed with a low-speed spin (1,000 × *g* for 1 min). The immunocomplexes were recovered through two serial elutions. For each, 10 μl of boiling-hot SDS sample buffer was added, followed by light vortexing, a 5-min incubation at room temperature, and centrifugation (1,000 × *g* for 2 min) into a fresh 96-well plate. Twelve microliters of each sample was loaded onto a 26-well 4–15% gradient Criterion SDS/PAGE gel (Bio-Rad) along with prestained Magic Mark (Invitrogen) and ^{14}C-methylated (GE Healthcare) protein molecular weight markers. Gels were run for 1 h at 200 V, and proteins were transferred to nitrocellulose for 90 min at 1.2 A in 20 mM NaH_2PO_4, pH 6.8. The membranes were exposed to a PhosphorImager screen (GE Healthcare) for 24–48 h, scanned on a Storm PhosphorImager (GE Healthcare), and analyzed by using IMAGEQUANT software.

Kinase reactions in the primary screen exhibited variable levels of background signal (e.g., see Fig. 5, which is published as supporting information on the PNAS web site), and thus had to be scored manually. Subsequent to the primary screen and deconvolution of the pools, we were able to drastically reduce the background signal in our assay (see Fig. 6, which is published as supporting information on the PNAS web site) by employing epoxy-coated magnetic beads (Dynal Biotech, Oslo) conjugated to human IgG (Sigma).

Pool Deconvolution. To deconvolute the pools, kinase assays were performed on each strain in each positive pool. Strains were grown and lysed as described above, but the final lysates came from 10-ml cultures of each strain.

Immunoblotting. Immunoblots were probed with an antibody raised against the calmodulin-binding peptide region of the TAP-tag (6) (Open Biosystems; no. CAB1001). We used a horseradish peroxidase-linked goat anti-rabbit IgG secondary antibody (Bio-Rad). The membranes were treated with Supersignal West Femto Maximum Sensitivity Substrate (Pierce) and visualized by using a charge-coupled device camera (Alpha Innotech, San Leandro, CA).

Tobacco Etch Virus (TEV) Protease Cleavage Kinase Assay. Kinase assays were performed on identical aliquots of extract for each candidate as described above, except that the final kinase concentration was 30 nM, and immunoprecipitation was performed with epoxy-coated magnetic beads conjugated to human IgG. After the immunoprecipitation, the beads were resuspended in 15 μl of IP buffer with or without 2 μl of TEV protease (10 units/μl, Invitrogen). Proteolysis proceeded for 30 min at 25°C with constant agitation. Samples were then boiled in sample buffer and analyzed as above.

Kinase Specificity Assays. Pho85(F82G)–Pcl1 and Pho85(F82G)–Pho80 were each used at a final concentration of 30 nM in parallel kinase reactions on identical aliquots of TAP-tagged strain extracts. Substrates were immunoprecipitated with human IgG-coupled magnetic beads and analyzed as described above. Bands were quantitated by using GE Healthcare IMAGEQUANT software. Similar results were obtained when the reactions were performed with 3 nM kinase.

Determining Kinetic Constants. Because our reactions were carried out in the presence of ATP, the sensitivity of our assay is largely dependent on the nucleotide selectivity of the kinase. We determined the kinetic constants for wild-type and AS Pho85–Pho80 by using both ATP and N^6-benzyl-ATP and found that the mutant kinase has ≈6.5-fold preference for N^6-benzyl-ATP (Table 2, which is published as supporting information on the PNAS web site). A previous study using an AS version of Cdc28 reported a 130-fold preference for the analog over ATP (5), suggesting that other kinases may produce greater sensitivity in this assay than Pho85. Kinase reaction time courses were measured with 1 nM Pho85–Pho80 or Pho85(F82G)–Pho80, 5.2 μM Pho4, and 5 μCi of radiolabeled nucleotide over a range of total nucleotide concentrations at 30°C in 10% glycerol/50 mM Tris·HCl, pH 7.5/150 mM NaCl/10 mM MgCl$_2$/1 mM DTT/ 0.01% Nonidet P-40/1 mM PMSF/2.5 mM benzamidine/0.1 mg/ml BSA. V_{max} and K_m were determined from Lineweaver–Burk plots of the initial rates of phosphorylation and the nucleotide concentrations. We calculated k_{cat} from V_{max} assuming that 100% of the enzyme was active.

Determining the Limits of Detection. Kinase reactions were performed with 10 nM Pho85(F82G)–Pho80 or Pho4-TAP extracts diluted with *pho4* deletion strain extracts. Parallel reactions were performed by using dilutions of purified Pho4 protein fused to the same affinity tag present at the C terminus of the TAP-tag along with dilutions of a quadruple serine-to-alanine Pho4 mutant (9) that can only be singly phosphorylated. Immunoblots were used to assign absolute protein abundance values to the Pho4-TAP samples based on the levels of recombinant Pho4. Signals >2× the background were considered detectable.

Results and Discussion

To screen 4,250 strains (Fig. 1), each expressing a single protein epitope-tagged with the TAP tag (21), we grew cells from each
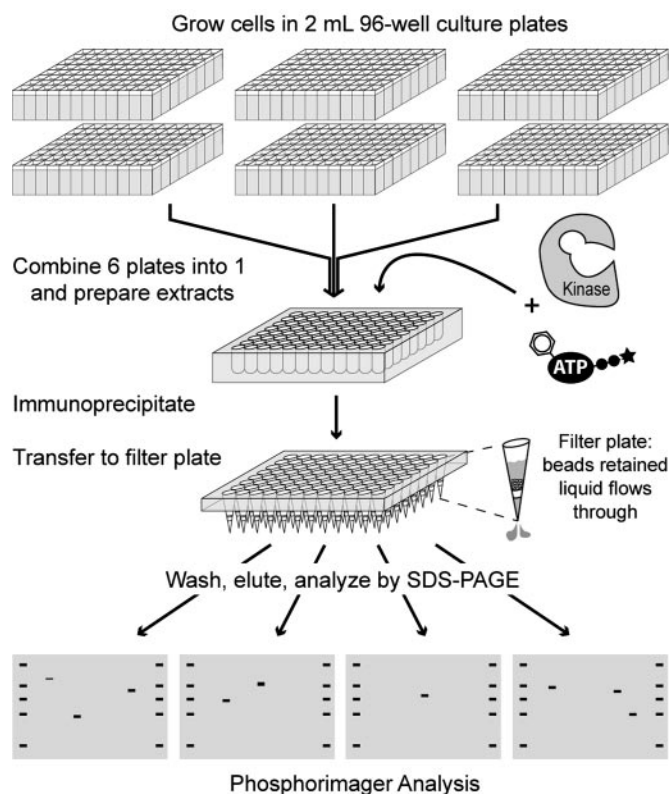
Fig. 1. Strategy for chemical genetic screening of the yeast proteome for kinase substrates. TAP-tagged strains were grown in 96-well plates, pooled, and lysed. Kinase reactions were performed by adding purified analog-specific kinase and radiolabeled ATP analog to the extracts. The tagged proteins were isolated by immunopurification, separated by gel electrophoresis, transferred to a membrane, and analyzed on a PhosphorImager.

strain in 96-well plates to late-logarithmic phase and combined pellets from cultures of six different strains before cell lysis (7). Kinase reactions were started by adding Pho85(F82G)–Pcl1 kinase produced in *E. coli* to yeast extracts along with ^{32}P-labeled N^6-benzyl-ATP. Tagged proteins were isolated by immunopurification (7), resolved on SDS/polyacrylamide gels, transferred to nitrocellulose, and exposed to a PhosphorImager screen for analysis. The same membranes were then immunoblotted for the TAP tag. All bands with radioactive signals above background were scored as positive. The complete screen of all 4,250 strains yielded 55 pools with a positive signal (representative positive results are shown in Fig. 5). Analysis of the immunoblots from one plate of reactions revealed that we successfully immunoprecipitated 86% of the library proteins (data not shown), indicating that most proteins (including many highly abundant ones) are not phosphorylated in the assay (for examples of negative results from individual strain assays see Fig. 5).

To eliminate spurious signals and to identify the proteins corresponding to the bands in the pooled extracts, we screened each of the individual strains in the positive pools (Fig. 5). Deconvolution of these 55 pools revealed 34 positive strains.

Because the immunopurifications were performed in nondenaturing conditions, it was not possible to distinguish between signals arising from the tagged protein and those from coprecipitating, untagged proteins. To determine which of these proteins were direct substrates of Pho85–Pcl1, we took advantage of the protease cleavage sequence in the TAP tag (21). This sequence is specifically recognized and cleaved by the TEV protease and lies N terminal to the dual protein A domains in the tag. If the radiolabeled protein visible from the PhosphorImager
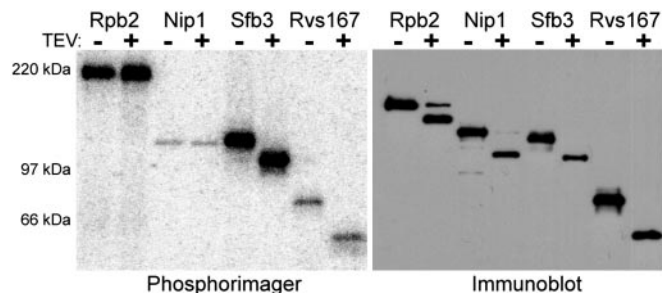
Fig. 2. TEV protease cleavage assay to identify direct substrates. Kinase reactions and immunopurifications were performed in duplicate and either treated with TEV protease (right lane of each pair) or mock-treated (left lane) after immunopurification. The reaction products were separated on polyacrylamide gels, transferred to a membrane, scanned on a PhosphorImager (*Left*), and immunoblotted for the TAP tag (*Right*). A shift in the electrophoretic mobility of the radiolabeled band on protease treatment indicates that the phosphorylated protein contains the TEV protease recognition sequence and, therefore, that the TAP-tagged protein is a direct substrate.

scan is the TAP-tagged protein, cleavage and release of the protein A domains will result in an increase in electrophoretic mobility visible on the PhosphorImager scan. We repeated reactions for the 34 positive strains in duplicate, adding TEV protease to one set of reactions after immunopurification and mock-treating the others. Twenty-four of our 34 targets showed a change in electrophoretic mobility upon TEV protease treatment (Fig. 2 and data not shown), indicating that they were direct targets of Pho85–Pcl1 (Table 1). Additionally for these 24 proteins, the signals from the radiolabeled band and those detected by immunoblotting comigrated. The 10 strains showing no shift in the radiolabeled band upon TEV cleavage displayed clearly shifted signals upon immunoblotting the cleaved products (Fig. 2 and data not shown), indicating that the TEV protease cleavage reaction proceeded to completion and that the radiolabeled protein and the tagged protein are different species.

The Pho85 cyclins are believed to direct Pho85 kinase to different substrates (22). In support of this idea, none of the Pcls can substitute for the function of Pho80 in phosphorylating the transcription factor Pho4 *in vivo* (17). This specificity is recapitulated *in vitro* in extract kinase assays as well as in reactions with purified components. In both cases, we observe that Pho80–Pho85 phosphorylates Pho4 with dramatically higher efficiency than do Pcl1–Pho85 and Pcl7–Pho85 (Figs. 3 and 6; and N.D., unpublished results). Pho4 interacts directly with Pho80, which recruits this substrate to the kinase (17, 23). Rvs167, a putative substrate for Pcl2–Pho85, also physically interacts with Pcl2 (24), suggesting that direct physical interaction between the Pho85-associated cyclins and substrates may mediate substrate specificity. This mechanism for enhancing kinase specificity is also used by other CDKs involved in cell cycle progression (25). It is also likely that subcellular localization of Pcl–Pho85 complexes contributes to the selection of correct substrates. Pho80–Pho85 is localized exclusively to the nucleus, where it phosphorylates its substrate, Pho4 (26). Pcl1 is localized partially to the nucleus but is also found at the incipient bud site (27). The closely related cyclin Pcl2 is found at both of these sites as well as at the growing bud tip and bud neck (27).

To investigate the specificity of Pcl1–Pho85 for the candidate substrates, we compared the relative ability of Pho85–Pho80 and Pho85–Pcl1 to phosphorylate each substrate in parallel kinase assays on identical aliquots of extracts derived from TAP-tagged strains (Figs. 3 and 6). We observed three classes of substrates: Pho85–Pcl1-specific, those phosphorylated equally well by both kinases, and Pho85–Pho80-specific. Eight proteins were better phosphorylated by Pho85–Pcl1. Two proteins, Vip1 and Smp2,

Table 1. TEV protease cleavage-confirmed substrates

Protein	Description [yeast proteome database][†]
Pho85-Pcl1 specific substrates	
Dma1	Regulation of spindle position and septin ring assembly
Isr1	Protein kinase, inhibits staurosporine resistance
Pan3	Pab1-dependent ribonuclease
Kcc4	Protein kinase, associates with the septin ring
Rom2	Rho1 GEF, actin organization, cell polarity, cell wall integrity
Shs1	Septin ring component
Sfb3	CopII coat protein, Pma1 transport
Rvs167	Amphiphysin homolog, actin polarization
Pho85–Pho80 specific substrates	
Pho81*	Pho85/Pho80 cyclin dependent kinase inhibitor
Glc8*	Glc7 phosphatase regulatory subunit
Pho4*	Transcription factor, phosphate starvation response
Vip1	Actin organization and biogenesis
Smp2	Respiration, plasmid maintenance
Substrates phosphorylated by both kinases	
Ame1	COMA complex member, functions in kinetochore assembly
Bcp1	Export of Mss4 and 60S ribosomal subunit components
Gts1	Regulator of metabolic oscillations
Cdc19	Pyruvate kinase
Ksp1	Protein kinase, suppressor of *prp20–10*
Npl3	mRNA binding protein, mRNA nuclear export
Pam1	Multicopy suppressor of *pph21-Δ*, *pph22-Δ*, *sit4-Δ* lethality
Reg1	Glc7 phosphatase regulatory subunit
Rpg1	eIF3 translation initiation factor subunit
Sap185	Sit4 phosphatase regulatory protein
Ssd1	Cell wall organization and biogenesis, suppressor of *sit4-Δ*
Ugp1	UDP-glucose phosphorylase, glycogen and glucan synthesis
YFR017C	Unknown
YNR047W	Protein kinase, suppresses α-factor-induced arrest

*Pho81, Glc8, and Pho4 were identified in a pilot screen using Pho80/85.
†Ref. 48.

were better phosphorylated by Pho85–Pho80. Three additional proteins, identified in a pilot screen by using Pho85–Pho80 kinase, were also tested in this assay and showed a marked specificity for Pho85–Pho80. Fourteen of our candidates showed no significant specificity for either kinase. *In vivo*, conditions not preserved in our assay, such as subcellular localization, may contribute to specificity, or it may be that these proteins are more specifically phosphorylated by another Pho85-cyclin complex. The high degree of specificity observed for many of the newly identified substrates suggests that they may be bona fide *in vivo* targets of Pho85–Pcl1 and Pho85–Pho80.

The cyclins Cln1, Cln2, Pcl1, and Pcl2 are essential for proper septin ring dynamics and cellular polarization (27). These functions are consistent with the localization of Pcl1 and Pcl2 proteins to the incipient bud site, the growing bud tip, and the bud neck. In a recent genome-wide localization analysis, 124 of the 4,156 (3%) proteins assigned a localization were found at the bud neck and/or in the bud (28). Twenty-two of the candidate substrates we identified have known cellular localizations. Five of them (Shs1, Pam1, Kcc4, Rpg1, and Rom2) (≈23%) are found at the bud or bud neck (28–32), >7-fold more than would be expected by random sampling. Among the five bud neck and bud
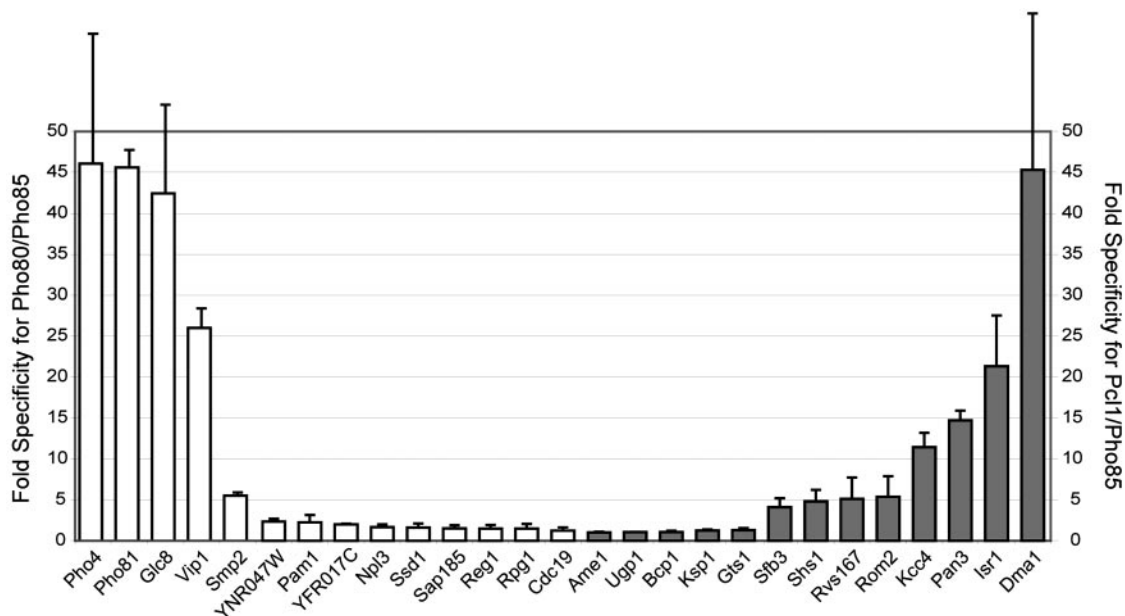
BIOCHEMISTRY

Fig. 3. Kinase-substrate specificity; relative activity of Pho85–Pho80 and Pho85–Pcl1 toward each substrate. Kinase reactions were performed on identical aliquots of each extract with Pho85(F82G)–Pho80 or Pho85(F82G)–Pcl1 kinase and analyzed as before. Fold specificity is defined as the ratio of the larger signal to the smaller for each substrate. Open bars, Pho85(F82G)–Pho80 signal/Pho85(F82G)–Pcl1 signal; filled bars, Pho85(F82G)–Pcl1 signal/Pho85(F82G)–Pho80 signal. Data shown are the averages of at least three experiments for each pair of reactions, and the error bars represent the mean ± standard deviation.

localized substrates are three of the six Pcl1-specific substrates, including a structural component of the septin ring and known regulators of septin dynamics and actin polarization. An additional target, Dma1, plays a role in septin ring assembly (33). Colocalization of these substrates and Pcl1–Pho85 further suggests that the substrates we have identified are specific for this kinase.

Synthetic lethal screens with *pho85* have revealed a number of functional groups of Pho85-interacting genes, implying roles for Pho85 in the processes these gene products control (34, 35). Genes whose products are involved in cell wall formation, maintenance, and regulation, including members of the PKC/ mitogen-activated protein (MAP) kinase cell integrity sensing pathway, constitute the largest of the Pho85 synthetic lethal gene classifications. Of the 24 direct substrates (Table 1), 7 have known roles in cell wall formation, maintenance, and regulation

(36–40) and/or interact with elements of the PKC/MAP kinase pathway (41–46) (Fig. 4). The second-largest group of genes synthetically lethal with *pho85* act in polarized cell growth. Eight of the 24 substrates we identified are among 314 genes classified in the Munich Information Center for Protein Sequences (MIPS) Functional Catalog under the closely related heading "Budding, Cell Polarity, and Filament Formation" (47) (Fig. 4 *Left*). It is also notable that 4 of the 8 budding, cell polarity, and filament formation candidates (Kcc4, Rom2, Rvs167, and Shs1) are Pcl1-specific substrates and that Pcl1 localizes to sites of polarized cell growth (27). The high degree of functional overlap between Pho85 and the identified proteins further suggests that many of them will prove to be true substrates. Further characterization of these targets will likely help to better define the role of Pho85–Pcl1 in the cell cycle and in cell polarization. For example, Kcc4, Rom2, and Shs1 may represent downstream
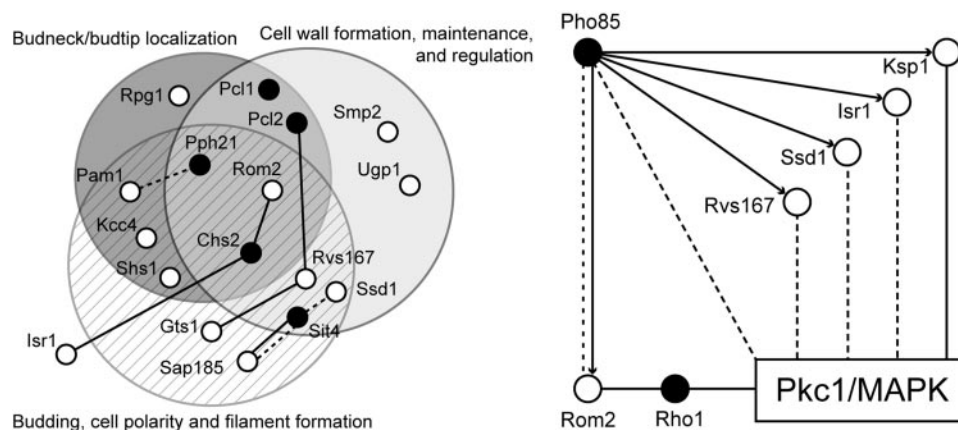

Fig. 4. Functional and spatial overlap between Pho85 and substrates. (*Left*) Venn diagram showing some of the substrates that function in Pho85-related processes and/or that colocalize with Pcl1, Pcl2. Additional genetic and physical interactions are indicated. (*Right*) Network diagram depicting interactions between Pho85, its substrates, and the PKC/mitogen-activated protein (MAP) kinase pathway. ○, Pho85 substrate; ●, nonsubstrate protein; solid line, physical interaction; dashed line, genetic interaction; →, kinase–substrate interaction.

effectors of Pho85-Pcl1 that help it carry out its essential function in the absence of Cln1 and Cln2 (11).

One of the challenges in adapting methods to a proteomic scale is maintaining sufficient sensitivity. Despite using only ≈2 OD_{600} units of cells, we were able to detect many proteins of extremely low abundance, including seven present in <1,000 copies per cell and an eighth whose expression was too low to be detected without immunoprecipitation (6). Despite our ability to identify a number of low-abundance proteins, we likely missed some substrates that fell below the limits of detection or that were obscured by the variable background signal. Four proteins have been reported to be phosphorylated in a Pho85-dependent manner and can be phosphorylated by Pho85–Pcl1 kinase *in vitro* (Rvs167, Gcn4, Cdc24, and Sic1). Only one of these proteins, Rvs167, was identified in our screen. We assayed the others and observed no signal for Gcn4 and very weak phosphorylation for Cdc24 and Sic1 (data not shown). These proteins may have been missed because of their low abundance. Alternatively, they may not be bona fide Pho85–Pcl1 substrates. During the course of our work, we were able to improve our assay by using a different bead system that nearly eliminated the background signal (compare the gels in Figs. 5 and 6). Using this system and dilutions of recombinant Pho4, we measured the detection limits of our assay. The assay can reliably detect singly phosphorylated proteins that are present in 800 copies per cell from <2 ml of logarithmic-phase culture (data not shown). Pho4-TAP, which can be multiply phosphorylated, was detectable at the equivalent of 200 copies per cell (data not shown). Using this bead system, finding ways to forgo the use of pools, and increasing the amount and/or quality of extract will further increase sensitivity in future screens.

We have demonstrated a rapid and sensitive method to identify protein kinase substrates by using full-length proteins at natural abundance levels. The ability of this assay to identify known substrates of Pho85 kinases, the functional overlap between the identified targets and Pho85–Pcl1, and the colocalization of the targets and kinase suggest that many of them will prove to be true *in vivo* substrates. This method is readily adaptable to other yeast kinases and with modifications can be used to screen for substrates in other systems.

1. Berwick, D. C. & Tavare, J. M. (2004) *Trends Biochem. Sci.* **29,** 227–232.
2. Manning, B. D. & Cantley, L. C. (2002) *Sci. STKE* **162,** PE49.
3. Liu, Y., Shah, K., Yang, F., Witucki, L. & Shokat, K. M. (1998) *Chem. Biol.* **5,** 91–101.
4. Shah, K. & Shokat, K. M. (2002) *Chem. Biol.* **9,** 35–47.
5. Ubersax, J. A., Woodbury, E. L., Quang, P. N., Paraz, M., Blethrow, J. D., Shah, K., Shokat, K. M. & Morgan, D. O. (2003) *Nature* **425,** 859–864.
6. Ghaemmaghami, S., Huh, W. K., Bower, K., Howson, R. W., Belle, A., Dephoure, N., O'Shea, E. K. & Weissman, J. S. (2003) *Nature* **425,** 737–741.
7. Howson, R., Huh, W. K., Ghaemmaghami, S., Falvo, J. V., Bower, K., Belle, A., Dephoure, N., Wykoff, D. D., Weissman, J. S. & O'Shea, E. K. (2005) *Comp. Funct. Genomics* **6,** 2–16.
8. Lenburg, M. E. & O'Shea, E. K. (1996) *Trends Biochem. Sci.* **21,** 383–387.
9. Komeili, A. & O'Shea, E. K. (1999) *Science* **284,** 977–980.
10. Measday, V., Moore, L., Ogas, J., Tyers, M. & Andrews, B. (1994) *Science* **266,** 1391–1395.
11. Espinoza, F. H., Ogas, J., Herskowitz, I. & Morgan, D. O. (1994) *Science* **266,** 1388–1391.
12. Moffat, J., Huang, D. & Andrews, B. (2000) *Prog. Cell Cycle Res.* **4,** 97–106.
13. Huang, D., Moffat, J., Wilson, W. A., Moore, L., Cheng, C., Roach, P. J. & Andrews, B. (1998) *Mol. Cell. Biol.* **18,** 3289–3299.
14. Carroll, A. S., Bishop, A. C., DeRisi, J. L., Shokat, K. M. & O'Shea, E. K. (2001) *Proc. Natl. Acad. Sci. USA* **98,** 12578–12583.
15. Jeffery, D. A., Springer, M., King, D. S. & O'Shea, E. K. (2001) *J. Mol. Biol.* **306,** 997–1010.
16. Edelhoch, H. (1967) *Biochemistry* **6,** 1948–1954.
17. Kaffman, A., Herskowitz, I., Tjian, R. & O'Shea, E. K. (1994) *Science* **263,** 1153–1156.
18. Kaffman, A., Rank, N. M. & O'Shea, E. K. (1998) *Genes Dev.* **12,** 2673–2683.
19. Kraybill, B. C., Elkin, L. L., Blethrow, J. D., Morgan, D. O. & Shokat, K. M. (2002) *J. Am. Chem. Soc.* **124,** 12118–12128.
20. Haswell, E. S. & O'Shea, E. K. (1999) *Mol. Cell. Biol.* **19,** 2817–2827.
21. Rigaut, G., Shevchenko, A., Rutz, B., Wilm, M., Mann, M. & Seraphin, B. (1999) *Nat. Biotechnol.* **17,** 1030–1032.
22. Carroll, A. S. & O'Shea, E. K. (2002) *Trends Biochem. Sci.* **27,** 87–93.
23. Byrne, M., Miller, N., Springer, M. & O'Shea, E. K. (2004) *J. Mol. Biol.* **335,** 57–70.
24. Lee, J., Colwill, K., Aneliunas, V., Tennyson, C., Moore, L., Ho, Y. & Andrews, B. (1998) *Curr. Biol.* **8,** 1310–1321.
25. Loog, M. & Morgan, D. O. (2005) *Nature* **434,** 104–108.
26. Kaffman, A., Rank, N. M., O'Neill, E. M., Huang, L. S. & O'Shea, E. K. (1998) *Nature* **396,** 482–486.
27. Moffat, J. & Andrews, B. (2004) *Nat. Cell Biol.* **6,** 59–66.
28. Huh, W. K., Falvo, J. V., Gerke, L. C., Carroll, A. S., Howson, R. W., Weissman, J. S. & O'Shea, E. K. (2003) *Nature* **425,** 686–691.
29. Mino, A., Tanaka, K., Kamei, T., Umikawa, M., Fujiwara, T. & Takai, Y. (1998) *Biochem. Biophys. Res. Commun.* **251,** 732–736.
30. Barral, Y., Parra, M., Bidlingmaier, S. & Snyder, M. (1999) *Genes Dev.* **13,** 176–187.
31. Hasek, J., Kovarik, P., Valasek, L., Malinska, K., Schneider, J., Kohlwein, S. D. & Ruis, H. (2000) *Cell Motil. Cytoskeleton* **45,** 235–246.
32. Manning, B. D., Padmanabha, R. & Snyder, M. (1997) *Mol. Biol. Cell* **8,** 1829–1844.
33. Fraschini, R., Bilotta, D., Lucchini, G. & Piatti, S. (2004) *Mol. Biol. Cell* **15,** 3796–3810.
34. Lenburg, M. E. & O'Shea, E. K. (2001) *Genetics* **157,** 39–51.
35. Huang, D., Moffat, J. & Andrews, B. (2002) *Mol. Cell. Biol.* **22,** 5076–5088.
36. Daran, J. M., Dallies, N., Thines-Sempoux, D., Paquet, V. & Francois, J. (1995) *Eur. J. Biochem.* **233,** 520–530.
37. Lussier, M., White, A. M., Sheraton, J., di Paolo, T., Treadwell, J., Southard, S. B., Horenstein, C. I., Chen-Weiner, J., Ram, A. F., Kapteyn, J. C., *et al.* (1997) *Genetics* **147,** 435–450.
38. Kaeberlein, M. & Guarente, L. (2002) *Genetics* **160,** 83–95.
39. Bickle, M., Delley, P. A., Schmidt, A. & Hall, M. N. (1998) *EMBO J.* **17,** 2235–2245.
40. Breton, A. M., Schaeffer, J. & Aigle, M. (2001) *Yeast* **18,** 1053–1068.
41. Uesono, Y., Toh-e, A. & Kikuchi, Y. (1997) *J. Biol. Chem.* **272,** 16103–16109.
42. Ozaki, K., Tanaka, K., Imamura, H., Hihara, T., Kameyama, T., Nonaka, H., Hirano, H., Matsuura, Y. & Takai, Y. (1996) *EMBO J.* **15,** 2196–2207.
43. Miyahara, K., Hirata, D. & Miyakawa, T. (1998) *Biosci. Biotechnol. Biochem.* **62,** 1376–1380.
44. Ho, Y., Gruhler, A., Heilbut, A., Bader, G. D., Moore, L., Adams, S. L., Millar, A., Taylor, P., Bennett, K., Boutilier, K., *et al.* (2002) *Nature* **415,** 180–183.
45. Tong, A. H., Lesage, G., Bader, G. D., Ding, H., Xu, H., Xin, X., Young, J., Berriz, G. F., Brost, R. L., Chang, M., *et al.* (2004) *Science* **303,** 808–813.
46. Bon, E., Recordon-Navarro, P., Durrens, P., Iwase, M., Toh-e, A. & Aigle, M. (2000) *Yeast* **16,** 1229–1241.
47. Ruepp, A., Zollner, A., Maier, D., Albermann, K., Hani, J., Mokrejs, M., Tetko, I., Guldener, U., Mannhaupt, G., Munsterkotter, M. & Mewes, H. W. (2004) *Nucleic Acids Res.* **32,** 5539–5545.
48. Costanza, M. C., Hogan, J. D., Cusick, M. E., Davis, B. P., Fancher, A. M., Hodges, P. E., Kondu, P., Lengieza, C., Lew-Smith, J. E., Lingner, C., *et al.* (2000) *Nucleic Acids Res.* **28,** 73–76.

BIOCHEMISTRY